JOURNAL OF AGRICULTURAL AND FOOD CHEMISTRY

New Analytical Methods

A novel dimethylhydrazine-derived spirolactam fluorescent chemodosimeter for tracing basal ONOO- in live cells and zebrafish

Caiyun Liu, Xue Zhang, Zilu Li, Yanan Chen, Zihan Zhuang, Pan Jia, Hanchuang Zhu, Yamin Yu, Baocun Zhu, and Wenlong Sheng

J. Agric. Food Chem., **Just Accepted Manuscript** • DOI: 10.1021/acs.jafc.9b01298 • Publication Date (Web): 14 May 2019

ACS Publications

is published by the American Chemical Society. 1155 Sixteenth Street N.W., Washington, DC 20036

A novel dimethylhydrazine-derived spirolactam fluorescent chemodosimeter for tracing basal $ONOO^-$ in live cells and zebrafish

Caiyun Liu,[†,*] Xue Zhang,[†] Zilu Li,[†] Yanan Chen,[†] Zihan Zhuang,[†] Pan Jia,[†] Hanchuang Zhu,[†] Yamin Yu,[†] Baocun Zhu,[†,*] and Wenlong Sheng [‡,*]

[†] School of Water Conservancy and Environment, University of Jinan, Jinan 250022, China.

[‡] Biology Institute, Qilu University of Technology (Shandong Academy of Sciences), Jinan 250103, China.

*Corresponding author. Fax: +86-531-82767617; Tel.: +86-531-82767617

E-mail address: liucaiyun1982072@163.com (C. Liu), lcyzbc@163.com (B. Zhu) and 15618694162@163.com (W. Sheng)

ABSTRACT

The precise cellular function of peroxynitrite ($ONOO^-$) in biosystems remains elusive, primarily owing to be short of ultrasensitive techniques for monitoring its intracellular distribution. In this work, a novel rhodamine B cyclic 1,2-dimethylhydrazine fluorescent chemodosimeter **RDMH-PN** for highly specific and ultrasensitive monitoring of basal $ONOO^-$ in biosystems was rationally designed. The fluorescence titration experiments demonstrated that **RDMH-PN** was capable of quantitatively detecting 0-100 nM $ONOO^-$ (LOD = 0.68 nM). In addition, **RDMH-PN** has the outstanding performances of ultrafast measurement, naked-eye detection, and preeminent selectivity toward $ONOO^-$ to accurately detect intracellular basal $ONOO^-$. Finally, it has been confirmed that **RDMH-PN** not only could map the intracellular basal $ONOO^-$ level by inhibit tests, but also could trace the fluctuations of endogenous and exogenous $ONOO^-$ levels with diverse stimulations in live cells and zebrafish.

KEYWORDS: fluorescent chemodosimeter; peroxynitrite ($ONOO^-$); 1,2-dimethylhydrazine; rhodamine; fluorescence bioimaging

INTRODUCTION

Peroxynitrite ($ONOO^-$), an important reactive oxygen species (ROS), is formed by a diffusion-limited coupling of NO and $O_2^{\bullet -}$ at the rate of 50-100 μM per min in biological systems, and can be stable and last for hours in the nanomolar concentration range.[1-3] Peroxynitrite plays crucial roles in signal transduction and antibacterial activities.[4,5] However, growing evidence has suggested that excessively produced $ONOO^-$ can damage various biomacromolecules because of its powerful oxidative and nitrative capbility.[6,7] An increasing number of diseases have been proved to be closely associated with $ONOO^-$, such as neurodegenerative disease, chronic inflammation, and cardiovascular disorders.[8-11] Unfortunately, the exact cellular mechanisms of $ONOO^-$ are still not completely disclosed because of being short of ultrasensitive techniques for monitoring its intracellular distribution. Therefore, developing accurate and ultrasensitive methods for visualizing the ultralow concentration $ONOO^-$ in the complex biosystems is urgently needed.

The expanding emergence of $ONOO^-$ fluorescent chemodosimeters shows their extraordinary superiority in measuring exogenous and endogenous $ONOO^-$ in biosystems.[12-36] It is because that fluorescent chemodosimeters not only hold unique imaging features of high spatiotemporal resolution, *in situ* detection, and non-invasiveness, but also possess excellent selectivity because they are mainly designed based on their specific reaction with target analytes.[37-42] Up to now, available $ONOO^-$ fluorescent chemodosimeters are mainly constructed based on different reactive recognition moieties, including *N*-phenylrhodol,[26-27] boronic acid pinacol ester,[30-34] electron-poor C=C double bond,[43-49] ketoamide,[50-52] hydrazine,[53-58] organoselenium,[59] and organotellurium.[60] However, almost all fluorescent chemodosimeters for tracing intracellular $ONOO^-$ suffer from the interferences of

other ROS (e.g. H_2O_2 and OCl^-) due to their similar properties.[61-66] On the other hand, most of available fluorescent chemodosimeters only detect enhanced concentration intracellular $ONOO^-$ because of their low sensitivity and high reactivity, short half-life, ultralow basal concentration of $ONOO^-$. Therefore, developing specific fluorescent chemodosimeters for accurately tracing intracellular basal $ONOO^-$ without the interferences of other ROS remains a great challenge.

In this work, a simple fluorescent chemodosimeter employing 1,2-dimethylhydrazine as novel reactive recognition receptor was prepared for highly specific and sensitive detection of $ONOO^-$. Experimental results demonstrated that the as-synthesized chemodosimeter not only hold prominent specificity for $ONOO^-$ than other relevant species including ROS, but also can accurately detect nanomolar concentration $ONOO^-$ with ultrafast response speed (< 3 s). The satisfactory biocompatibility enables it to trace intracellular basal $ONOO^-$ and the fluctuations of exogenous/endogenous $ONOO^-$ levels with various stimulations in live cells and zebrafish. More importantly, the dimethylhydrazine-derived spirolactam has been proven to be a unique model for constructing highly specific and ultrasensitive chemodosimeters for $ONOO^-$.

EXPERIMENTAL SECTION

General information. The chemicals and instrumentations are displayed in Supporting Information. The fluorescence and absorption spectra were determined 1 minute after various species addition at 25 °C except for kinetics experiments. The stock solution of chemodosimeter **RDMH-PN** was prepared in DMSO and the adopted analytical condition is the PBS solution containing 5% DMSO (20 mM, pH = 7.4).

Preparation of chemodosimeter **RDMH-PN.** Phosphorus oxychloride (459 mg,

3 mmol) were dissolved in absolute 1,2-dichloroethane (10 mL). Then, rhodamine B (479 mg, 1 mmol) was introduced into the above mixture and refluxed for 4 hours. After removing the solvent, the solution of 1,2-dimethylhydrazine dihydrochloride (133 mg, 1 mmol) and DIPEA (1.349g, 10 mmol) in absolute CH_2Cl_2 (15 mL) was added slowly to the above residue. The resulted mixture was further reacted at 25 ˚C for another 12 hours. After removing CH_2Cl_2, the crude products were refined through silica gel chromatography to afford chemodosimter **RDMH-PN** (296 mg, 61%). ^{1}H-NMR (400 MHz, $CDCl_3$) δ (ppm): 1.16(t, *J* = 7.2 Hz, 12H), 2.31(s, 3H), 2.79(s, 3H), 3.28-3.42(m, 8H), 6.29(dd, *J* = 2.8, 8.8 Hz, 2H), 6.51(d, *J* = 2.4 Hz, 2H), 6.71(d, *J* = 8.4 Hz, 2H), 7.30(d, *J* = 6.4 Hz, 1H), 7.48-7.56(m, 2H), 8.25(dd, *J* = 1.6, 7.2 Hz, 1H); ^{13}C-NMR (100 MHz, $CDCl_3$) δ (ppm): 12.58, 34.60, 38.86, 44.42, 63.33, 99.10, 106.27, 110.03, 127.37, 127.69, 129.03, 130.09, 130.29, 132.20, 137.95, 148.55, 154.21, 164.10. HRMS (ESI): Calcd for $C_{30}H_{37}N_4O_2$ $[M+H]^+$ 485.2911; Found, 485.2913.

RESULTS AND DISCUSSION

Design of chemodosimeter RDMH-PN. An excellent fluorescent chemodosimeter is the perfect combination of eminent fluorophore and unique reactive recognition receptor. Xanthenes have been extensively applied in exploring fluorescent chemodosimeters for various target analytes owing to the outstanding photophysical properties including high fluorescence quantum yield, negligible cytotoxicity, and the unique easy-regulation of ring-opening of the corresponding non-fluorescent spirolactam.[67-69] Based on the above-mentioned description, screening appropriate reactive recognition unit is essential for constructing a specific and ultrasensitive $ONOO^-$ fluorescent chemodosimeters. Recently, a large number of hydrazide-based fluorescent chemodosimeters have been successfully constructed for

identifying $ONOO^-$.[53-58] But the selectivity and reaction activity of those chemodosimeters toward $ONOO^-$ are closely associated with the adopted fluorophores,[56,66] and especially the hydrazide-containing spirolactams are prone to be hydrolyzed with the catalysis of Cu^{2+}.[67-69] Therefore, to further optimize the response properties of such chemodosimeters, a novel fluorescent chemodosimeter for $ONOO^-$ detection was proposed by replacing hydrazide moiety with 1,2-dimethylhydrazine recognition group. Namely, the newly designed chemodosimeter was composed of rhodamine B dye as fluorophore and 1,2-dimethylhydrazine as the reactive unit (**RDMH-PN**, Scheme 1 and 2). The 1,2-dimethylhydrazine group was integrated into fluorophore, which formed spirocyclic ring system to reduce the fluorescence. Upon the addition of $ONOO^-$, chemodosimeter **RDMH-PN** causes the ring-opening reaction, and leads to the recovery of fluorescence.[61-65] The design and reaction mechanism has been also verified by HPLC and HRMS (Fig. S1-S2).

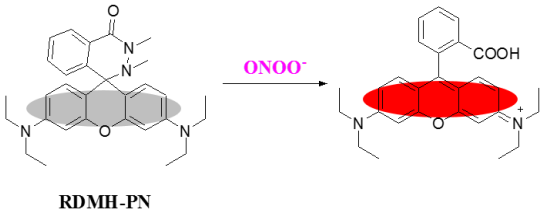

Scheme 1. Recognition mechanism of chemodosimter **RDMH-PN** for $ONOO^-$ detection.

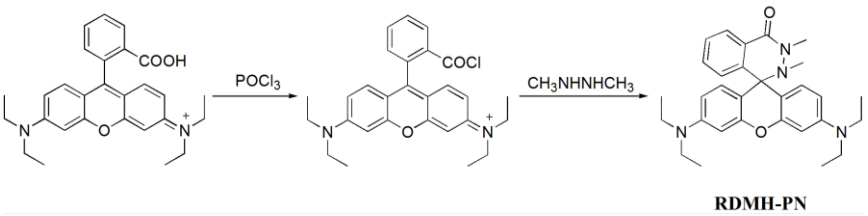

Scheme 2. Preparation of chemodosimter **RDMH-PN**.

Determination of $ONOO^-$. Firstly, fluorescence spectra of **RDMH-PN** with $ONOO^-$ were obtained in the PBS solution (20 mM, pH 7.4, 5% DMSO). As depicted in Figure 1a, chemodosimeter **RDMH-PN** solution emitted negligible fluorescence.

As designed, the emission peak was enhanced gradually with $ONOO^-$ (0-10 μM). Satisfactorily, increasing $ONOO^-$ concentrations (1-10 μM) manifest a linear enhancement of the **RDMH-PN** fluorescence intensity (linear equation: $y = 286942 \times [ONOO^-]$ (μM) + 235185, $R^2 = 0.9907$) (Figure 1b). Furthermore, to estimate the capability of **RDMH-PN** to detect extremely low concentration $ONOO^-$, the additional titration of $ONOO^-$ in the range of ultralow concentration was implemented. Excitedly, the favorable linear dependence between fluorescence intensities and $ONOO^-$ concentrations ranging from 0-100 nM was also obtained, demonstrating chemodosimeter **RDMH-PN** could accurately determine $ONOO^-$ at the nanomolar level (Figure 1c). Subsequently, the limit of detection was determined to be 0.68 nM (3σ/k). Furthermore, the ultrafast reaction (< 3 s) between **RDMH-PN** and 1 equiv. $ONOO^-$ has been confirmed in Figure 2. These spectral studies revealed that chemodosimeter **RDMH-PN** has powerful capability to implement the real-time determination of highly reactive $ONOO^-$ with excellent sensitivity (Table S1).

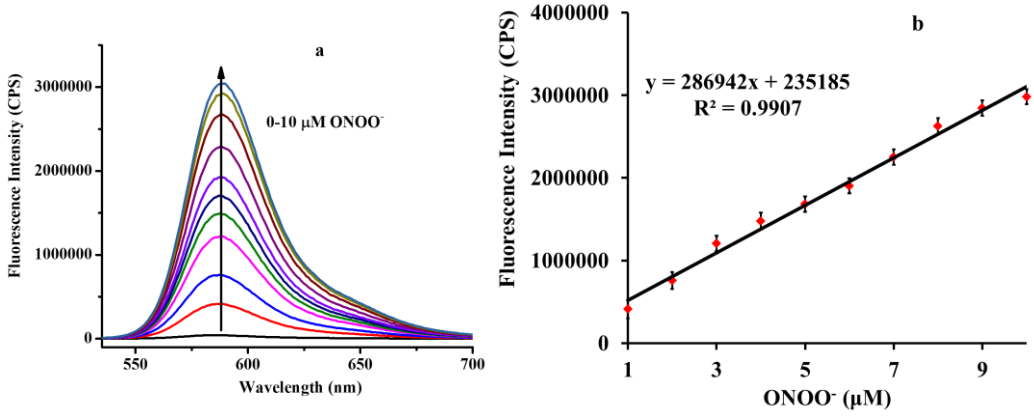

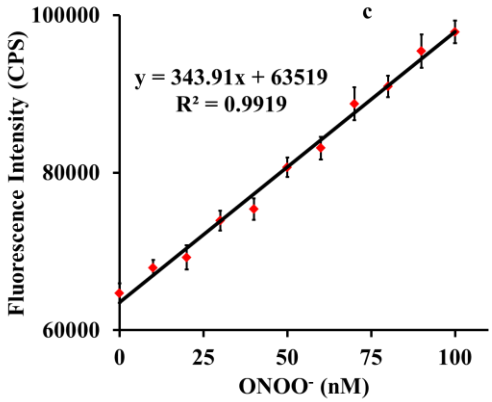

Figure 1. (a) Concentration-dependent fluorescent spectra of **RDMH-PN** (5 μM) with different concentration $ONOO^-$ (0-10 μM) under the PBS solution (20 mM, pH = 7.4, 5% DMSO). (b) The linear dependence between fluorescence intensities and $ONOO^-$ concentrations (1-10 μM). (c) The linear dependence between fluorescence intensities and $ONOO^-$ concentrations (0-100 nM). λ_{ex} = 520 nm. Slit widths: W_{ex} = W_{em} = 3 nm. The spectra were recorded in 1 min after $ONOO^-$ injection at 25 °C.

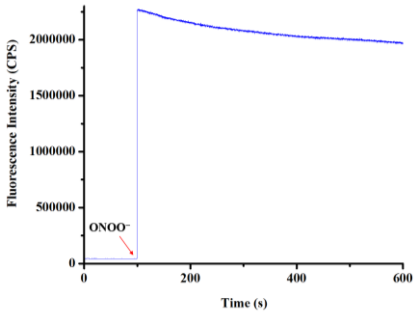

Figure 2. Time-course of **RDMH-PN** (5 μM) with $ONOO^-$ (5 μM) under the PBS solution (20 mM, pH = 7.4, 5% DMSO). λ_{ex} = 520 nm, λ_{em} = 585 nm. Slit widths: W_{ex} = W_{em} = 3 nm. This experiment was performed at 25 °C.

The absorption spectrum of chemodosimter **RDMH-PN** for determining $ONOO^-$ was also estimated in the PBS solution (20 mM, pH 7.4, 5% DMSO). Chemodosimter **RDMH-PN** (5 μM) displayed negligible absorption intensity before reacting with $ONOO^-$. As predicted, the reaction between chemodosimter **RDMH-PN** and $ONOO^-$

led to clear enhancement of absorption intensity at 570 nm. Color change of **RDMH-PN** could be distinctly observed with and without $ONOO^-$, which was beneficial to naked-eye observation.

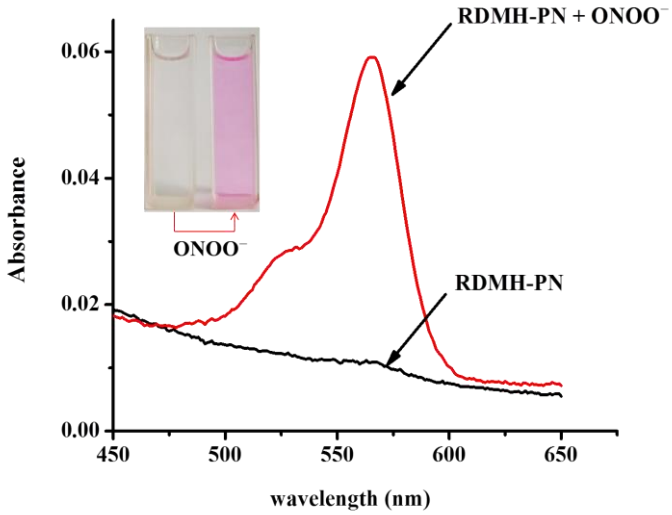

Figure 3. Absorption spectra of **RDMH-PN** (5 μM) with/without $ONOO^-$ (5 μM) under the PBS solution (20 mM, pH = 7.4, 5% DMSO). Inset: photos of the **RDMH-PN** (20 μM) solution with/without $ONOO^-$ (20 μM). The spectra were recorded in 1 min after $ONOO^-$ injection at 25 °C.

These results manifested the usability of chemodosimter **RDMH-PN** as an ultrafast quantitative tool for monitoring $ONOO^-$ at ultralow concentration level under physiological conditions. The above-mentioned recognition properties of **RDMH-PN** make it convenient to trace intracellular basal $ONOO^-$.

Specificity of chemodosimeter RDMH-PN toward $ONOO^-$. The specificity of **RDMH-PN** has been verified in the presence of $ONOO^-$ and other relevant analytes including K^+, Na^+, Ca^{2+}, Mg^{2+}, Cu^{2+}, Cu^+, Fe^{2+}, Fe^{3+}, Zn^{2+}, Br^-, SO_3^{2-}, CO_3^{2-}, NO_3^-, NO_2^-, NO, TBHP, H_2O_2, $^{\bullet}O^tBu$, $^{\bullet}OH$, O_2^-, $^1O_2$, Cys, Hcy, GSH, OCl^-, and $ONOO^-$.

As shown in Figure 4, only $ONOO^-$ induced a significant increment of fluorescence intensity at 585 nm, and other analytes could not cause the obvious changes of fluorescence intensity. Subsequently, the possible interferences of pH on chemodosimeter **RDMH-PN** for monitoring $ONOO^-$ were also studied. These results manifested that chemodosimeter **RDMH-PN** possessed a satisfactory stability and response capability for $ONOO^-$ in the physiological pH ranges (Fig. S3). Moreover, the eminent photo-stability of chemodosimeter **RDMH-PN** was further proven (Fig. S4). The above consequences implied chemodosimeter **RDMH-PN** could accurately trace intracellular $ONOO^-$ in the bioimaging applications.

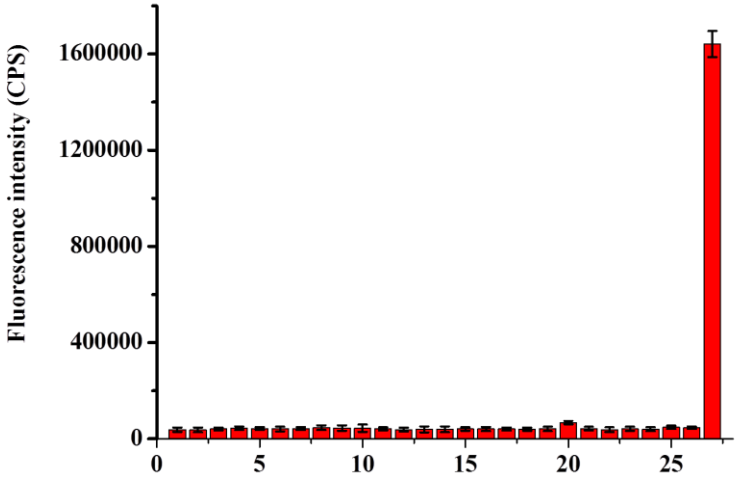

Figure 4. Fluorescence changes of **RDMH-PN** (5 μM) with various species (100 μM except for annotations) under the PBS solution (20 mM, pH = 7.4, 5% DMSO). 1. Blank, 2. K^+ (1 mM), 3. Na^+ (1 mM), 4. Ca^{2+} (1 mM), 5. Mg^{2+} (1 mM), 6. Cu^{2+}, 7. Cu^+, 8. Fe^{2+}, 9. Fe^{3+}, 10. Zn^{2+}, 11. Br^-, 12. SO_3^{2-}, 13. CO_3^{2-}, 14. NO_3^-, 15. NO_2^-, 16. NO, 17. TBHP, 18. H_2O_2 (500 μM), 19. $^{\bullet}O^tBu$, 20. $^{\bullet}OH$, 21. O_2^-, 22. $^1O_2$, 23. Cys (500 μM), 24. Hcy (500 μM), 25. GSH (1 mM), 26. OCl^-, and 27. $ONOO^-$ (5 μM). λ_{ex} =

520 nm, λ_{em} = 585 nm. Slit widths: W_{ex} = W_{em} = 3 nm. The spectra were recorded in 1 min after analytes injection at 25 °C.

Bioimaging of $ONOO^-$ in live cells. To study the recognition properties of chemodosimeter **RDMH-PN** for $ONOO^-$ in complex living systems, we conducted biological imaging experiments with RAW 264.7 macrophages. Initially, we checked the cytotoxicity of chemodosimeter **RDMH-PN** by a cell counting kit-8 (CCK-8) method. These results displayed chemodosimeter **RDMH-PN** had negligible effect on cell survival (Figure 5). Then, we followed to test whether chemodosimeter **RDMH-PN** has capability to trace intracellular basal $ONOO^-$. Firstly, the bioimaging of control cells was carried out, and almost no intracellular fluorescence was observed (Figure 6a-c). As predicted, the macrophages preincubated with chemodosimeter **RDMH-PN** for 30 minutes exhibited the obvious red intracellular fluorescence under the same bioimaging conditions (Figure 6d-f). Additionally, the macrophages pretreated with 4-amino-tempo (a superoxide scavenger, it causes the reduction of intracellular $ONOO^-$ levels) was further treated with chemodosimeter **RDMH-PN** for 30 minutes, and the weaker red intracellular fluorescence than the control macrophages incubated with only **RDMH-PN** was observed (Fig. S5). These data demonstrated chemodosimeter **RDMH-PN** was quite sensitive to basal $ONOO^-$ in normal macrophages without extrinsic stimuli. Subsequently, the macrophages preincubated with chemodosimeter **RDMH-PN** for 30 minutes were further treated with $ONOO^-$ (20 μM) for another 20 minutes, and the stronger intracellular fluorescence was successfully obtained (Figure 6g-i), demonstrating chemodosimeter

RDMH-PN could determine the changes of exogenous $ONOO^-$ concentrations. To estimate the capability of **RDMH-PN** in detecting endogenous $ONOO^-$, the macrophages were stimulated by PMA (1.0 μg/mL) and LPS (1.0 μg/mL) for 30 minutes. With extending incubation with **RDMH-PN** for another 20 minutes, a significant increase of intracellular fluorescence has been observed (Figure 6j-l). Above results demonstrated that chemodosimeter **RDMH-PN** could map the basal $ONOO^-$ and the changes of endogenous/exogenous $ONOO^-$ concentrations in live macrophages effectively (Figure 6m).

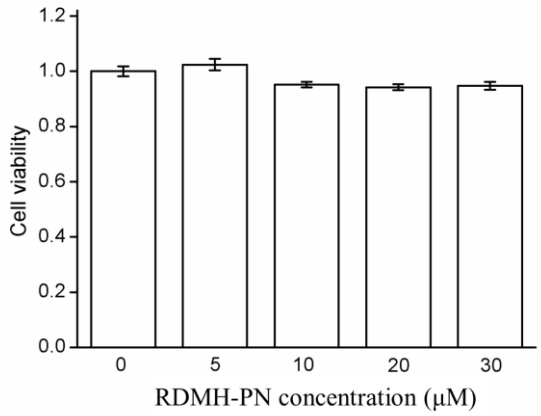

Figure 5. Macrophage viability with different concentration chemodosimeter **RDMH-PN**.

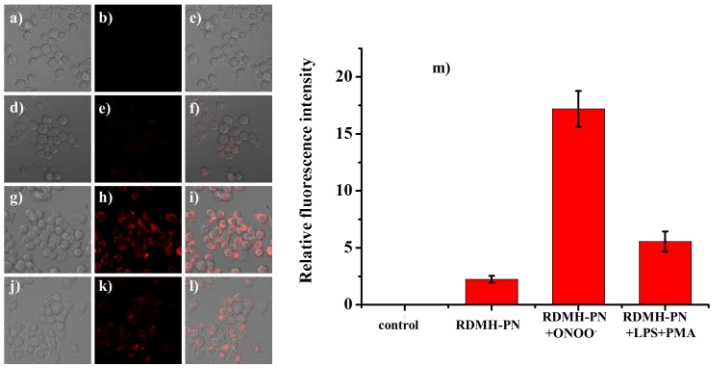

Figure 6. Fluorescence images of live macrophages: (a-c) control cells; (d-f) cells treated with **RDMH-PN**; (g-i) cells preincubated with **RDMH-PN**, and then treated

with $ONOO^-$; (j-l) cells preincubated with LPS and PMA, and then incubated **RDMH-PN**; (m) the fluorescence intensities of the corresponding cells.

Bioimaging of $ONOO^-$ in zebrafish. With the favorable bioimaging performance of **RDMH-PN** in live cells, we then examined whether it has the possibility to bioimage $ONOO^-$ in vivo. Based on this consideration, the 4-day-old zebrafish was chosen as a suitable organism model to visualize basal $ONOO^-$ and the changes of endogenous/exogenous $ONOO^-$ concentrations in our experiments (Figure 7). Firstly, the bioimaging of control zebrafish was carried out, and almost no fluorescence was observed (Figure 7a-c). As designed, the zebrafish preincubated with chemodosimeter **RDMH-PN** for 30 minutes exhibited the obvious red fluorescence under the same bioimaging conditions (Figure 7d-f). These results indicated chemodosimeter **RDMH-PN** was very sensitive to basal $ONOO^-$ in normal zebrafish without extrinsic stimuli. Subsequently, the zebrafish preincubated with chemodosimeter **RDMH-PN** for 30 minutes was further treated with $ONOO^-$ (50 μM) for another 20 minutes, and the stronger red fluorescence was also successfully obtained (Figure 7g-i), demonstrating chemodosimeter **RDMH-PN** could monitor the changes of exogenous $ONOO^-$ levels in vivo. Moreover, to estimate the capability of **RDMH-PN** in detecting endogenous $ONOO^-$ in vivo, the zebrafish were stimulated by PMA (1.0 μg/mL) and LPS (1.0 μg/mL) for 30 minutes. With extending incubation with **RDMH-PN** for another 20 minutes, the significant increase of fluorescence also confirmed the bioimaging applicability in vivo (Figure 7j-l). Taking all these results in consideration, it can be concluded that chemodosimeter **RDMH-PN** was able to

accurately monitor intracellular basal $ONOO^-$ and the changes of endogenous/exogenous $ONOO^-$ concentrations in zebrafish.

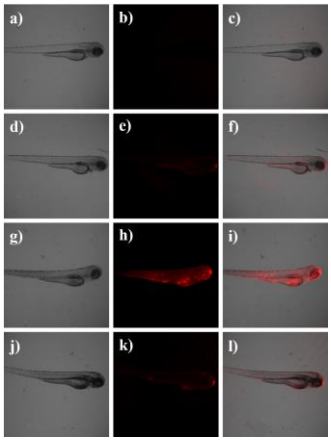

Figure 7. Fluorescence images of zebrafish: (a-c) control zebrafish; (d-f) zebrafish treated with **RDMH-PN**; (g-i) zebrafish preincubated with **RDMH-PN**, and then treated with $ONOO^-$; (j-l) zebrafish preincubated with LPS and PMA, and then incubated **RDMH-PN**.

In conclusion, we have constructed a novel fluorescent chemodosimeter for tracing intracellular basal $ONOO^-$ in biosystems. The high specificity and ultrasensitivity of chemodosimeter **RDMH-PN** was ascribed to the adoption of reactive recognition group of 1,2-dimethylhydrazine. Bioimaging applications of chemodosimeter **RDMH-PN** in tracing intracellular basal $ONOO^-$ and the changes of $ONOO^-$ concentrations with different stimulations in live cells and zebrafish were confirmed. Therefore, we anticipate that chemodosimeter **RDMH-PN** may be used as a powerful tool to explore the generation and transport of $ONOO^-$ in biosystems. Moreover, the 1,2-dimethylhydrazine modified spirocyclic structure has been proven to be a unique model for constructing highly specific and ultrasensitive chemodosimeters for $ONOO^-$ detection.

ASSOCIATED CONTENT

*****Supporting Information

The Supporting Information is available free of charge on the ACS Publications website at DOI: 10.1021/acs.jafc.×××××××.

Experimental methods and additional data.

Notes

The authors declare no competing financial interest.

ACKNOWLEDGEMENTS

This study was financially supported by NSFC (21777053 and 21607053) and Shandong Provincial Natural Science Foundation (ZR2017MB014).

REFERENCES

(1) Szabo, C.; Ischiropoulos, H.; Radi, R. Peroxynitrite: biochemistry, pathophysiology and development of therapeutics. *Nat. Rev. Drug Discov*. **2007**, *6*, 662-680.

(2) Radi, R.; Beckman, J. S.; Bush K. M.; Freeman, B. A. Peroxynitrite oxidation of sulfhydryls. The cytotoxic potential of superoxide and nitric oxide. J. Biol. Chem. **1991**, *266 (7)*, 4244-4250.

(3) Goldstein, S.; Lind, J.; Merényi, G. Chemistry of peroxynitrites as compared to peroxynitrates. *Chem. Rev.* **2005**, *105*, 2457-2470.

(4) Alvarez, M. N.; Peluffo, G.; Piacenza, L.; Radi, R. Intraphagosomal peroxynitrite as a macrophage-derived cytotoxin against internalized trypanosoma cruzi: consequences for oxidative killing and role of microbial peroxiredoxins in

infectivity. *J. Biol. Chem.* **2011**, *286*, 6627-6640.

(5) Liaudet, L.; Vassalli, G.; Pacher, P. Role of peroxynitrite in the redox regulation of cell signal transduction pathways. *Front. Biosci., Landmark Ed.* **2009**, *14*, 4809-4814.

(6) Ascenzi, P.; di Masi, A.; Sciorati, C.; Clementi, E. Peroxynitrite—An ugly biofactor? *BioFactors* **2010**, *36*, 264-273.

(7) Radi, R. Peroxynitrite, a stealthy biological oxidant. *J. Biol. Chem.* **2013**, *288*, 26464-26472.

(8) Dickinson, B. C.; Chang, C. J. Chemistry and biology of reactive oxygen species in signaling or stress responses. *Nat. Chem. Biol.* **2011**, *7*, 504-511.

(9) Pacher, P.; Beckman, J. S.; Liaudet, L. Nitric oxide and peroxynitrite in health and disease. *Physiol. Rev.* **2007**, *87*, 315-424.

(10) Dickinson, B. C.; Srikun, D.; Chang, C. J. Mitochondrial-targeted fluorescent probes for reactive oxygen species. *Curr. Opin. Chem. Biol.* **2010**, *14*, 50-56.

(11) Szabó, C.; Ischiropoulos, H.; Radi, R. Peroxynitrite: biochemistry, pathophysiology and development of therapeutics. *Nat. Rev. Drug Discov.* **2007**, *5*, 662-680.

(12) Li, D.; Wang, S.; Lei, Z.; Sun, C.; El-Toni, A. M.; Alhoshan, M. S.; Fan, Y.; Zhang F. Peroxynitrite activatable NIR-II fluorescent molecular probe for drug-induced hepatotoxicity monitoring. *Anal. Chem.* **2019**, *91*, 4771-4779.

(13) Li, L.; Zan, M.; Qie, X.; Yue, J.; Miao, P.; Ge, M.; Wang, Z. C.; Bai, F.-Q.; Zhang, H. X.; Ferri, J. K.; Dong, W. F. Theoretical study on the photoinduced electron

transfer mechanisms of different peroxynitrite probes. *J. Phys. Chem. A* **2018**, *122*, 217-223.

(14) Zhu, B.; Wang, Z.; Zhao, Z.; Shu, W.; Zhang, M.; Wu, L.; Liu, C.; Duan, Q.; Jia, P. A simple highly selective and sensitive hydroquinone-based two-photon fluorescent probe for imaging peroxynitrite in live cells. *Sens. Actuators B* **2018**, *262*, 380-385.

(15) Cheng, D.; Pan, Y.; Wang, L.; Zeng, Z.; Yuan, L.; Zhang, X.; Chang, Y. T. Selective visualization of the endogenous peroxynitrite in an inflamed mouse model by a mitochondria-targetable two-photon ratiometric fluorescent probe. *J. Am. Chem. Soc.* **2017**, *139*, 285-292.

(16) Zhang, W.; Liu, Y.; Gao,Q.; Liu, C.; Song, Bo.; Zhang. R.; Yuan, J. A ruthenium(II) complex–cyanine energy transfer scaffold based luminescence probe for ratiometric detection and imaging of mitochondrial peroxynitrite. Chem. Commun. **2018**, *54*, 13698-13701.

(17) Shen, Y.; Zhang, X.; Zhang, Y.; Li, H.; Dai, L.; Peng, X.; Peng, Z.; Xie, Y. A fluorescent sensor for fast detection of peroxynitrite by removing of C=N in a benzothiazole derivative. *Anal. Chim. Acta* **2018**, *1014*, 71-76.

(18) Cheng, P.; Zhang, J.; Huang, J.; Miao, Q.; Xu, C.; Pu, K. Near-infrared fluorescence probes to detect reactive oxygen species for keloid diagnosis. *Chem. Sci.* **2018**, *9*, 6340-6347.

(19) Jiao, X. Y.; Li, Y.; Niu, J. Y.; Xie, X. L.; Wang, X.; Tang, B. Small-molecule fluorescent probes for imaging and detection of reactive oxygen, nitrogen, and

sulfur species in biological systems. *Anal. Chem.* **2018**, *90*, 533-555.

(20) Lee, D.; Lim, C.; Ko, G.; Kim, D.; Cho, M. K.; Nam, S.-J.; Kim, H. M.; Yoon, J. A two-photon fluorescent probe for imaging endogenous $ONOO^-$ near NMDA receptors in neuronal cells and hippocampal tissues. *Anal. Chem.* **2018**, *90*, 9347-9352.

(21) Hou, T.; Zhang, K.; Kang, X.; Guo, X.; Du, L.; Chen, X.; Yu, L.; Yue, J.; Ge, H.; Liu, Y.; Asirie, A. M.; Alamrye, K. A.; Yu, H.; Wang, S. Sensitive detection and imaging of endogenous peroxynitrite using a benzo thiazole derived cyanine probe. *Talanta* **2019**, *196*, 345-351.

(22) Li, Z.; Liu, R.; Tan, Z.-L.; He, L.; Lu, Z. L.; Gong, B. Aromatization of 9,10-dihydroacridine derivatives: discovering a highly selective and rapid-responding fluorescent probe for peroxynitrite. *ACS Sens.* **2017**, *2*, 501-505.

(23) Zhu, H.; Fan, J.; Du, J.; Peng, X. Fluorescent probes for sensing and imaging within specific cellular organelles. *Acc. Chem. Res.* **2016**, *49*, 2115-2126.

(24) Zhang, J.; Zhen, X.; Zeng, J.; Pu, K. A dual-modal molecular probe for near-infrared fluorescence and photoacoustic imaging of peroxynitrite. *Anal. Chem.* **2018**, *90*, 9301-9307.

(25) Sedgwick, A. C.; Han, H.-H.; Gardiner, J. E.; Bull, S. D.; He, X. P.; James, T. D. Long-wavelength fluorescent boronate probes for the detection and intracellular imaging of peroxynitrite. *Chem. Commun.* **2017**, *53*, 12822-12825.

(26) Peng, T.; Wong, N.-K.; Chen, X.; Chan, Y.-K.; Ho, D.; Sun, Z.; Hu, J. J.; Shen, J.;

El-Nezami, H.; Yang, D. Molecular imaging of peroxynitrite with HKGreen-4 in live cells and tissues. *J. Am. Chem. Soc.* **2014**, *136*, 11728-11734.

(27) Peng, T.; Chen, X.; Gao, L.; Zhang, T.; Wang, W.; Shen, J.; Yang, D. A rationally designed rhodamine-based fluorescent probe for molecular imaging of peroxynitrite in live cells and tissues. *Chem. Sci.* **2016**, *7*, 5407-5413.

(28) Wu, L.; Wang, Y.; Weber, M.; Liu, L.; Sedgwick, A. C.; Bull, S. D.; Huang, C.; James, T. D. ESIPT-based ratiometric fluorescence probe for the intracellular imaging of peroxynitrite. *Chem. Commun.* **2018**, *54*, 9953-9956.

(29) Li, J.-B.; Chen, L.; Wang, Q.; Liu, H.-W.; Hu, X.-X.; Yuan, L.; Zhang, X.-B. A bioluminescent probe for imaging endogenous peroxynitrite in living cells and mice. *Anal. Chem.* **2018**, *90*, 4167-4173.

(30) Yu, F.; Song, P.; Li, P.; Wang, B.; Han, K. A fluorescent probe directly detect peroxynitrite based on boronate oxidation and its applications for fluorescence imaging in living cells. *Analyst* **2012**, *137*, 3740-3749.

(31) Sedgwick, A. C.; Dou, W.-T.; Jiao, J.-B.; Wu, L.; Williams, G. T.; Jenkins, A. T. A.; Bull, S. D.; Sessler, J. L.; He, X.-P.; James, T. D. An ESIPT Probe for the ratiometric imaging of peroxynitrite facilitated by binding to Aβ-Aggregates. *J. Am. Chem. Soc.* **2018**, *140*, 14267-14271.

(32) Zhu, B.; Wu, L.; Wang, Y.; Zhang, M.; Zhao, Z.; Liu, C.; Wang, Z.; Duan, Q.; Jia, P. A highly selective and ultrasensitive ratiometric far-red fluorescent probe for imaging endogenous peroxynitrite in living cells. *Sens. Actuators B* **2018**, *259*, 797-802.

(33) Zhang, J.; Li, Y.; Zhao, J.; Guo, W. An arylboronate-based fluorescent probe for selective and sensitive detection of peroxynitrite and its applications for fluorescence imaging in living cells. *Sens. Actuators B* **2016**, *237*, 67-74.

(34) Palanisamya, S.; Wu, P.-Y.; Wu, S.-C.; Chen, Y.-J.; Tzou, S.-C.; Wang, C.-H.; Chen, C.-Y.; Wang, Y.-M. In vitro and in vivo imaging of peroxynitrite by a ratiometric boronate based fluorescent probe. *Biosens. Bioelectron.* **2017**, *91*, 849-856.

(35) Miao, J.; Huo, Y.; Shi, H.; Fang, J.; Wang, J.; Guo, W. A Si-rhodamine-based near-infrared fluorescent probe for visualizing endogenous peroxynitrite in living cells, tissues, and animals. *J. Mater. Chem. B* **2018**, *6*, 4466-4473.

(36) Peng, T.; Yang, D. HKGreen-3: A rhodol-based fluorescent probe for peroxynitrite. Org. Lett. 2010, 12, 4932-4935.

(37) Yang, Y. M.; Zhao, Q.; Feng, W.; Li, F. Y. Luminescent Chemodosimeters for Bioimaging. *Chem. Rev.* **2013**, *113*, 192-270.

(38) Li, X. H.; Gao, X. H.; Shi, W.; Ma, H. M. Design strategies for water-soluble small molecular chromogenic and fluorogenic probes. *Chem. Rev.* **2014**, *114*, 590-659.

(39) Ueno, T.; Nagano, T. Fluorescent probes for sensing and imaging. *Nat. Methods* **2011**, *8*, 642-645.

(40) Li, S.-J.; Zhou, D.-Y.; Li, Y.; Liu, H.-W.; Wu, P.; Ou-Yang, J.; Jiang, W.-L.; Li, C.-Y. Efficient two-photon fluorescent probe for imaging of nitric oxide during endoplasmic reticulum stress. *ACS Sens.* **2018**, *3*, 2311-2319.

(41) Ou-Yang, J.; Li, Y.; Jiang, W.-L.; He, S.-Y.; Liu, H.-W.; Li, C.-Y. Fluorescence-guided cancer diagnosis and surgery by a zero cross-talk ratiometric near-infrared γ-glutamyltranspeptidase fluorescent probe. *Anal. Chem.* **2019**, *91*, 1056-1063.

(42) Zhou, J.; Li, L.; Shi, W.; Gao, X.; Li, X.; Ma, H. HOCl can appear in the mitochondria of macrophages during bacterial infection as revealed by a sensitive mitochondrial-targeting fluorescent probe. *Chem. Sci.* **2015**, *6*, 4884-4888.

(43) Zhou, D.-Y.; Li, Y.; Jiang, W.-L.; Tian, Y.; Fei, J.; Li, C.-Y. A ratiometric fluorescent probe for peroxynitrite prepared by de novo synthesis and its application in assessing the mitochondrial oxidative stress status in cells and in vivo. *Chem. Commun.* **2018**, *54*, 11590-11593.

(44) Zhou, D.-Y.; Ou-Yang, J.; Li, Y.; Jiang, W.-L.; Tian, Y.; Yi, Z.-M.; Li, C.-Y. A ratiometric fluorescent probe for the detection of peroxynitrite with simple synthesis and large emission shift and its application in cells image. *Dyes Pigm.* **2019**, 161, 288-295.

(45) Zhou, D.-Y.; Li, Y.; Jiang, W.-L.; Tian, Y.; Fei, J.; Li, C.-Y. A ratiometric fluorescent probe for peroxynitrite prepared by de novo synthesis and its application in assessing the mitochondrial oxidative stress status in cells and in vivo. *Chem. Commun.* **2018**, *54*, 11590-11593.

(46) Guo, B.; Jing, J.; Nie, L.; Xin, F.; Gao, C.; Yang, W.; Zhang, X. A lysosome targetable versatile fluorescent probe for imaging viscosity and peroxynitrite

with different fluorescence signals in living cells. *J. Mater. Chem. B* **2018**, *6*, 580-585.

(47) Fu, Y.; Nie, H.; Zhang, R.; Xin, F.; Tian, Y.; Jing, J.; Zhang, X. An ESIPT based naphthalimide chemosensor for visualizing endogenous $ONOO^-$ in living cells. *RSC Adv.* **2018**, *8*, 1826-1832.

(48) Jia, X.; Chen, Q.; Yang, Y.; Tang, Y.; Wang, R.; Xu, Y.; Zhu, W.; Qian, X. FRET-based mito-specific fluorescent probe for ratiometric detection and imaging of endogenous peroxynitrite: dyad of Cy3 and Cy5. *J. Am. Chem. Soc.* **2016**, *138*, 10778-10781.

(49) Sun, W.; Shi, Y.-D.; Ding, A.-X.; Tan, Z.-L.; Chen, H.; Liu, R.; Wang, R.; Lu, Z.-L. Imaging viscosity and peroxynitrite by a mitochondria-targeting two-photon ratiometric fluorescent probe. *Sens. Actuators B* **2018**, *276*, 238-246.

(50) Li, Y.; Xie, X.; Yang, X.; Li, M.; Jiao, X.; Sun, Y.; Wang, X.; Tang, B. Two-photon fluorescent probe for revealing drug-induced hepatotoxicity via mapping fluctuation of peroxynitrite. *Chem. Sci.* **2017**, *8*, 4006-4011.

(51) Xie, X.; Tang, F.; Liu, G.; Li, Y.; Su, X.; Jiao, X.; Wang, X.; Tang, B. Mitochondrial peroxynitrite mediation of anthracycline-induced cardiotoxicity as visualized by a two-photon near-infrared fluorescent probe. *Anal. Chem.* **2018**, *90*, 11629-11635.

(52) Cheng, D.; Xu, W.; Yuan, L.; Zhang, X. Investigation of drug-induced hepatotoxicity and its remediation pathway with reaction-based fluorescent probes. *Anal. Chem.* **2017**, *89*, 7693-7700.

(53) Feng, W. Y.; Feng, G. Q. A lysosome-targetable fluorescent probe for imaging $ONOO^-$ in living cells and animals. *Dyes Pigm.* **2019**, *164*, 174-181.

(54) Feng, S. M.; Liu, D. D.; Feng, G. Q. A dual-channel probe with green and near-infrared fluorescence changes for in vitro and in vivo detection of peroxynitrite. *Anal. Chim. Acta* **2019**, *1054*, 137-144.

(55) Liu, D.; Feng, S.; Feng, G. A rapid responsive colorimetric and near-infrared fluorescent turn-on probe for imaging exogenous and endogenous peroxynitrite in living cells. *Sens. Actuators B* **2018**, *269*, 15-21.

(56) Wu, D.; Ryu, J.-C.; Chung, Y. W.; Lee, D.; Ryu, J.-H.; Yoon, J.-H.; Yoon, J. A far-red-emitting fluorescence probe for sensitive and selective detection of peroxynitrite in live cells and tissues. *Anal. Chem.* **2017**, *89*, 10924-10931.

(57) Li, Z.; Liu, C.; Yu, C.; Chen, Y.; Jia, P.; Zhu, H.; Zhang, X.; Yu, Y.; Zhu, B.; Sheng, W. highly selective and sensitive red-emitting fluorescent probe for visualization of endogenous peroxynitrite in living cells and zebrafish. *Analyst* **2019**, DOI: 10.1039/c9an00347a.

(58) Li, H.; Li, X.; Wu, X.; Shi, W.; Ma, H. Observation of the generation of $ONOO^-$ in mitochondria under various stimuli with a sensitive fluorescence probe. *Anal. Chem.* **2017**, *89*, 5519-5525.

(59) Yu, F.; Li, P.; Li, G.; Zhao, G.; Chu, T.; Han, K. A near-IR reversible fluorescent probe modulated by selenium for monitoring peroxynitrite and imaging in living cells. *J. Am. Chem. Soc.* **2011**, *133*, 11030-11033.

(60) Yu, F.; Li, P.; Wang, B.; Han, K. Reversible near-infrared fluorescent probe

introducing tellurium to mimetic glutathione peroxidase for monitoring the redox cycles between peroxynitrite and glutathione in vivo. *J. Am. Chem. Soc.* **2013**, *135*, 7674-7680.

(61) Dickinson, B. C.; Huynh, C.; Chang, C. J. A palette of fluorescent probes with varying emission colors for imaging hydrogen peroxide signaling in living cells. *J. Am. Chem. Soc.* **2010**, *132*, 5906-5915.

(62) Chan, J.; Dodani, S. C.; Chang, C. J. Reaction-based small-molecule fluorescent probes for chemo selective bioimaging. *Nat. Chem.* **2012**, *4*, 973-984.

(63) Yue, Y.; Huo, F.; Yin, C.; Escobedo, J. O.; Strongin, R. M. Recent progress in chromogenic and fluorogenic chemosensors for hypochlorous acid. *Analyst* **2016**, *141*, 1859-1873.

(64) Yin, C. X.; Huo, F. J.; Zhang, J. J.; Martínez-Máñez, R.; Yang, Y. T.; Lv, H. G.; Li, S. D. Thiol-addition reactions and their applications in thiol recognition. *Chem. Soc. Rev.* **2013**, *42*, 6032-6059.

(65) Xie, X.; Yang, X.; Wu, T.; Li, Y.; Li, M.; Tan, Q.; Wang, X.; Tang, B. Rational design of α-ketoamide-based near-infrared fluorescent probe specific for hydrogen peroxide in living systems. *Anal. Chem.* **2016**, *88*, 8019-8025.

(66) Zhang, R.; Zhao, J.; Han, G.; Liu, Z.; Liu, C.; Zhang, C.; Liu, B.; Jiang, C.; Liu, R.; Zhao, T.; Han, M.-Y.; Zhang, Z. Real-time discrimination and versatile profiling of spontaneous reactive oxygen species in living organisms with a single fluorescent probe. *J. Am. Chem. Soc.* **2016**, *138*, 3769-3778.

(67) Kim, H. N.; Lee, M. H.; Kim, H. J.; Kim, J. S.; Yoon, J. A new trend in

rhodamine-based chemosensors: application of spirolactam ring-opening to sensing ions. *Chem. Soc. Rev.* **2008**, *37*, 1465-1472.

(68) Chen, X.; Pradhan, T.; Wang, F.; Kim, J. S.; Yoon, J. Fluorescent chemosensors based on spiroring-opening of xanthenes and related derivatives. *Chem. Rev.* **2012**, *112*, 1910-1956.

(69) Dujols, V.; Ford, F.; Czarnik, A. W. A long-wavelength fluorescent chemodosimeter selective for Cu(II) ion in water. *J. Am. Chem. Soc.* **1997**, *119*, 7386-7387.

For TOC Only